PERGAMON

Deep-Sea Research II 46 (1999) 1745–1768

DEEP-SEA RESEARCH
PART II

Picophytoplankton dynamics and production in the Arabian Sea during the 1995 Southwest Monsoon

Susan L. Brown[a,*], Michael R. Landry[a], Richard T. Barber[b], Lisa Campbell[c], David L. Garrison[d], Marcia M. Gowing[e]

[a]*Department of Oceanography, University of Hawaii at Manoa, 1000 Pope Rd., Honolulu, HI 96822, USA*
[b]*NSOE, Duke University, Beaufort, NC 28516, USA*
[c]*Department of Oceanography, Texas A&M University, College Station, TX 77843, USA*
[d]*Division of Ocean Sciences, Biological Oceanography Program, National Science Foundation, 4201 Wilson Blvd. Arlington, VA 22230, USA*
[e]*Institute of Marine Sciences, University of California at Santa Cruz, Santa Cruz, CA 95064, USA*

Received 5 September 1997; received in revised form 1 December 1998; accepted 10 December 1998

Abstract

Phytoplankton community structure is expected to shift to larger cells (e.g., diatoms) with monsoonal forcing in the Arabian Sea, but recent studies suggest that small primary producers remain active and important, even in areas strongly influenced by coastal upwelling. To better understand the role of smaller phytoplankton in such systems, we investigated growth and grazing rates of picophytoplankton populations and their contributions to phytoplankton community biomass and primary productivity during the 1995 Southwest Monsoon (August–September). Environmental conditions at six study stations varied broadly from open-ocean oligotrophic to coastal eutrophic, with mixed-layer nitrate and chlorophyll concentrations ranging from 0.01 to 11.5 μM NO_3 and 0.16 to 1.5 μg Chl *a*. Picophytoplankton comprised up to 92% of phytoplankton carbon at the oceanic stations, 35% in the diatom-dominated coastal zone, and 26% in a declining *Phaeocystis* bloom. Concurrent in situ dilution and ^{14}C-uptake experiments gave comparable ranges of community growth rates (0.53–1.05 d^{-1} and 0.44–1.17 d^{-1}, to the 1% light level), but uncertainties in C:Chl *a* confounded agreement at individual stations. Microzooplankton grazing utilized 81% of community phytoplankton growth at the oligotrophic stations and 54% at high-nutrient coastal stations. *Prochlorococcus* (PRO) was present at two oligotrophic stations, where its maximum growth approached 1.4 d^{-1} (two doublings per day) and depth-integrated growth varied from

* Corresponding author.
E-mail address: sbrown@soest.hawaii.edu (S.L. Brown)

PII: S0967-0645(99)00042-9

0.2 to 0.8 d^{-1}. *Synechococcus* (SYN) growth ranged from 0.5 to 1.1 d^{-1} at offshore stations and 0.6 to 0.7 d^{-1} at coastal sites. Except for the most oligotrophic stations, growth rates of picoeukaryotic algae (PEUK) exceeded PRO and SYN, reaching 1.3 d^{-1} offshore and decreasing to 0.8 d^{-1} at the most coastal station. Microzooplankton grazing impact averaged 90, 70, and 86% of growth for PRO, SYN, and PEUK, respectively. Picoplankton as a group accounted for 64% of estimated gross carbon production for all stations, and 50% at high-nutrient, upwelling stations. Prokaryotes (PRO and SYN) contributed disproportionately to production relative to biomass at the most oligotrophic station, while PEUK were more important at the coastal stations. Even during intense monsoonal forcing in the Arabian Sea, picoeukaryotic algae appear to account for a large portion of primary production in the coastal upwelling regions, supporting an active community of protistan grazers and a high rate of carbon cycling in these areas.

1. Introduction

Extremely small cells, including the prokaryotic genera *Synechococcus* and *Prochlorococcus*, as well as picoplankton-sized eukaryotic algae (0.2–2.0 μm), are numerical and biomass dominants in the open oceans, where they contribute significantly to global primary production. In the equatorial Pacific Ocean, for example, picoplankton as a group account for 80–90% of chlorophyll a biomass, and prokaryotes (roughly, the less than 1 μm size fraction) contribute more than 50% of primary production (Chavez, 1989). In the vast subtropical oligotrophic regions of the open oceans, prokaryotic primary producers are even more important, accounting for up to 95% of ^{14}C uptake in surface waters (Glover, 1985; Iturriaga and Mitchell, 1986; Waterbury et al., 1986; Iturriaga and Marra, 1988). Based on nutrient enrichment and high phytoplankton biomass, the Arabian Sea is considered one of the most productive ocean systems; nevertheless, recent studies indicate that picoplankton may play a significant role in this rich system as well (Burkhill et al., 1993; Veldhuis et al., 1997; Reckermann and Veldhuis, 1997). An active and important community of small primary producers is also implied by relatively high rates of microzooplankton grazing, which utilize about half of the primary production in the upwelling region (Landry et al., 1998).

During the Southwest Monsoon, approximately June through September, southwest winds parallel to the Arabian coast produce a region of coastal upwelling that may extend 600–800 km offshore (Smith and Bottero, 1977; Elliott and Savidge, 1990; Brock and McClain, 1991; Young and Kindle, 1994). Further offshore, the wind stress curl reverses and open-ocean oligotrophic conditions prevail. These contrasting hydrographic regions represent an ideal situation for evaluating phytoplankton community responses in markedly differing environmental regimes. Increased nutrients during seasonal upwelling are expected to shift community structure to larger phytoplankton and thus greater potential export flux (Peinert et al., 1989; Michaels and Silver, 1988; Garrison et al., 1998). However, the effects of monsoonal forcing on the abundances, growth, production and fate of the smaller phytoplankton need to be better resolved to understand the partitioning of production between recycling

pathways and export flux. As part of the US JGOFS (Joint Global Ocean Flux Study) Arabian Sea Process Study, we investigated autotrophic picoplankton growth and mortality in conjunction with primary productivity experiments as measured by the uptake of ^{14}C-labeled bicarbonate. Concurrent in situ experiments during the 1995 Southwest Monsoon provide insight into the dynamics of component picoplankton populations, the picophytoplankton contribution to total production, and community growth rate inferences from different methods across a range of environmental conditions.

2. Materials and methods

Picophytoplankton growth, grazing losses and production were investigated in contemporaneous ^{14}C-uptake and dilution experiments at six stations in the Arabian Sea during the Southwest Monsoon, 1995 (Cruise TN050; August–September). These stations, representing a range of environmental conditions along the US JGOFS cruise track (Fig. 1, Table 1), were occupied for approximately two days each to allow for a full suite of sampling, experimental work, and to deploy and recover in situ arrays.

Seawater was collected between 0200 and 0300 h in 10-l Niskin bottles from eight depths corresponding to light penetration of 93, 75, 44, 27, 15, 7, 4, and 1% of incident photosynthetically active radiation (PAR_0). For each depth, ^{14}C-uptake and dilution experiments were prepared as described below. After experimental set-up, the incubation containers for each depth were mounted onto a clear Plexiglas rack, and each rack was clamped to the array line and returned to the approximate depth of sample

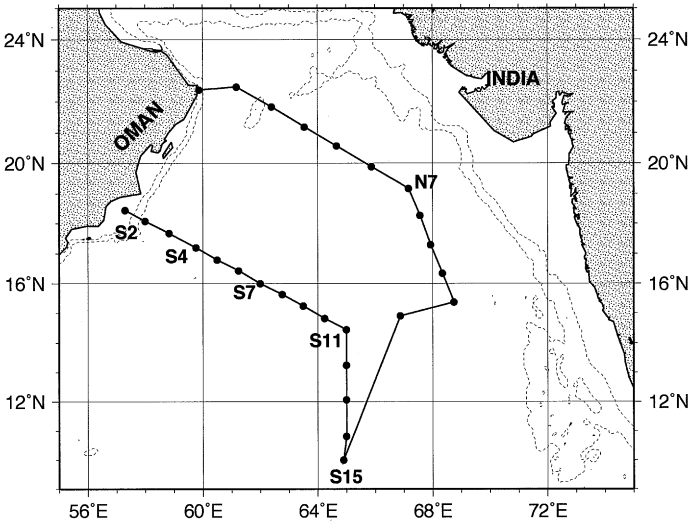

Fig. 1. Station locations for JGOFS Arabian Sea Process Study TN050.

Table 1
Summary of stations, depths, corresponding light levels, cell abundances, and environmental conditions for in situ incubation experiments in the Arabian Sea in August–September 1995 (TN050)

Station	Depth (m)	$\%I_0$	T(°C)	NO_3 (μM)	Chl *a* (μg l^{-1})	Abundances (10^3 cells ml^{-1})		
						PRO	SYN	PEUK
N7	1	93	27.9	0.01	0.17	163	80	2.6
N7	5	75	27.9	0.01	0.17	160	76	2.3
N7	13	44	27.9	0.01	0.16	151	74	2.8
N7	20	27	27.9	0.03	0.16	154	75	2.4
N7	30	15	27.9	0.01	0.16	164	74	2.3
N7	40	7	27.7	0.01	0.28	264	93	3.2
N7	50	4	27.1	7.20	0.75	100	8	5.5
N7	70	1	24.0	12.50	0.29	92	1	0.7
S15	1	93	27.8	0.14	0.22	260	52	3.1
S15	5	75	27.8	0.14	0.21	270	51	3.5
S15	15	44	27.8	0.17	0.22	263	50	3.6
S15	25	27	27.8	0.17	0.24	262	52	3.1
S15	35	15	27.8	0.21	0.22	276	51	3.3
S15	50	7	27.8	0.25	0.22	256	52	3.0
S15	60	4	27.8	0.28	0.22	270	54	2.8
S15	85	1	27.8	0.25	0.30	257	51	3.8
S11	0	100	27.1	0.01	1.32	1	45	3.8
S11	0	100	27.1	0.01	1.50	1	43	3.5
S11	1	90	27.1	0.05	1.41	1	42	3.5
S11	4	56	27.1	0.05	1.39	1	42	4.0
S11	10	29	27.1	0.04	1.11	1	41	3.8
S11	16	14	27.1	0.04	1.24	1	42	3.8
S11	22	8	27.1	0.06	1.24	1	44	3.7
S11	36	2	26.8	0.70	0.94	1	21	1.6
S7	1	93	26.6	2.80	0.92	3	123	8.5
S7	5	75	26.6	2.80	0.94	3	120	9.0
S7	10	44	26.6	2.80	0.94	3	119	8.3
S7	15	27	26.6	2.80	0.94	3	116	8.1
S7	20	15	26.6	2.80	0.94	3	118	7.4
S7	30	7	26.6	2.80	0.88	3	117	8.5
S7	38	4	26.6	2.80	0.95	2	115	8.2
S7	55	1	24.0	15.6	0.37	2	2	1.6
S4	1	93	25.0	8.90	0.57	1	51	13.1
S4	5	75	25.0	8.90	0.60	3	52	14.5
S4	10	44	25.0	9.00	0.72	3	52	13.1
S4	15	27	24.8	9.20	0.69	3	51	14.3
S4	20	15	24.6	9.60	0.89	5	43	12.9
S4	30	7	24.3	10.4	0.85	5	22	8.8
S4	38	4	24.0	11.70	0.43	2	7	3.3
S2	1	93	24.1	11.50	0.56	5	56	17.4
S2	3	75	24.1	11.50	0.57	3	56	17.3

Table 1 (Continued)

Station	Depth (m)	$\%I_0$	T(°C)	NO_3 (μM)	Chl *a* (μg l^{-1})	Abundances (10^3 cells ml^{-1})		
						PRO	SYN	PEUK
S2	8	44	24.1	11.50	0.60	2	55	18.8
S2	13	27	23.4	12.80	0.76	5	49	21.4
S2	19	15	22.6	14.80	0.78	5	38	20.5
S2	26	7	22.5	15.30	0.78	6	30	20.3
S2	32	4	21.6	16.60	1.03	5	21	16.7

collection. The in situ array was launched before dawn and held the bottles at a fixed depth throughout the natural daylight period. The bottles were recovered after approximately 12 h (after sunset), and the remainder of the 24-h incubation was completed in darkened incubators cooled with surface seawater. Rough seas prevented in situ incubations at station S11; consequently, the experiments at this station were conducted in shipboard incubators screened with blue Plexiglas and neutral density filters designed to approximate light levels and spectral quality at the depths of water collection.

2.1. ^{14}C-uptake experiments

^{14}C-uptake experiments were conducted in 270-ml polystyrene bottles that were rinsed three times with sample seawater and filled directly from the Niskin bottle without using a filling tube. The bottles were inoculated with 100 μl of ^{14}C-labeled sodium carbonate with a specific activity of 55 m Ci mmol^{-1}. Four bottles were prepared for in situ incubation at each depth, and occasionally an additional bottle was filled, inoculated, and filtered immediately to determine a time zero particulate ^{14}C blank. Two of the in situ bottles were processed as described below when the array was recovered, after approximately 12-h incubation during the natural photoperiod. The additional two bottles were processed after shipboard incubation in the dark for the remainder of the 24-h day. At the end of the incubations, 1-ml subsamples were taken from bottles at selected depths to determine the total added activity; these subsamples were added directly to scintillation vials containing beta-phenylethylamine (0.5 ml) and Ecolume scintillation fluid (10 ml). The contents of all bottles were filtered through 25-mm Whatman GF/F filters, and the filters were placed in scintillation vials, acidified with 0.5 ml of 0.5 N HCL, and allowed to ventilate under a hood for 24 h. Following the addition of 10 ml of Ecolume, the vials were stored in the dark for another 24 h before analysis with a shipboard liquid scintillation counter.

2.2. Dilution experiments

Small volume ("mini-") dilution experiments were designed to complement in situ primary production measurements by being fast and easy to prepare and attach to the

incubation array. Filtered seawater from each depth (from CTD bottles) was obtained by gravity filtration through an in-line filter capsule (Gelman Criticap, 0.2 μm). One dilution mixture for each depth was made by gently topping off a measured volume of whole seawater with the filtered water for a final mixture of 31% whole seawater. Replicate, acid-washed 53-ml polystyrene centrifuge tubes were thoroughly rinsed, then filled with either unfiltered seawater or the dilution mixture from each depth. Replicate initial 3-ml samples were taken from both the whole seawater and the dilution mixture for each depth, preserved in cryogenic tubes with paraformaldehyde (final concentration 1%) and frozen in liquid nitrogen for subsequent flow cytometric (FCM) analysis. Final 3-ml samples were taken for FCM analysis, and the remaining water in each tube was filtered onto a 25-mm Whatman GF/F glass-fibre filter for fluorometric analysis of chlorophyll *a*. Filters were extracted in 10 ml of 90% acetone for 24 h at 0°C. Concentrations of chlorophyll *a* were measured with a Turner Designs 10AU Field Fluorometer calibrated to HPLC-determined pigment concentrations.

FCM samples were thawed and stained with Hoechst 33342 (0.8 $\mu g\ ml^{-1}$ final concentration) for 30 min before analysis of picoplankton populations (Monger and Landry, 1993). Subsamples of 50–100 μl were enumerated on a Coulter EPICS 753 flow cytometer equipped with dual argon lasers and MSDS II automatic sampling. The lasers were aligned colinearly with the first laser tuned to the UV range to excite Hoechst-stained DNA. The blue fluorescence from the DNA stain was used to distinguish cells from nonliving particulate matter. The second laser was tuned to 488 nm at 1.3 W to excite the pigments of autotrophic cells. Picophytoplankton populations were distinguished from one another by differences in light scatter and fluorescence emission. *Synechococcus* spp. were identified primarily by strong orange (575 ± 40 nm) fluorescence (phycoerythrin). Cells of *Prochlorococcus* spp. were separated from similarly sized heterotrophic bacteria by the presence of red fluorescence (680 ± 40 nm) due to chlorophyll *a*. Picoeukaryotic algae were identified by higher forward and right-angle light scattering (indices of cell size) and enhanced red fluorescence compared to *Prochlorococcus*. All FCM samples were spiked with a mixture of Polysciences Fluoresbrite YG 0.57- and 0.98-μm visible beads and 0.46-μm UV beads. Changes in fluorescence per cell of the picoplankton populations within an experiment were normalized to the fluorescence values of the standard 0.57-μm beads.

2.3. Phytoplankton carbon estimates and c:chl ratios

Phytoplankton community carbon was estimated at each station from the combined contributions of populations enumerated by flow cytometry and microscopy. Flow cytometrically determined populations were converted to biomass equivalents using cellular carbon values of 53, 175 and 975 fg C $cell^{-1}$ for *Prochlorococcus* spp. (Campbell et al., 1994), *Synechococcus* spp. (Veldhuis et al., 1997) and picoeukaryotes (Reckermann and Veldhuis, 1997), respectively. The carbon values used are on the low end of estimates ranging up to 92 fg C $cell^{-1}$ for *Prochlorococcus* (Veldhuis et al., 1997) and 400 fg C $cell^{-1}$ for *Synechococcus* (Burkhill et al., 1993). The carbon content for picoeukaryotes is roughly intermediate between estimates of 225 and 2,108 fg C $cell^{-1}$ from Tarran et al. (1999) and Campbell et al. (1994), respectively.

Populations of larger phytoplankton were enumerated and sized as described by Garrison et al. (1998). Samples for these analyses were collected routinely at five depths (10, 25–30, 50, 75–80 and 100 m) from hydrocasts separate from, but closely following, the samplings for experimental setup. Autofluorescing flagellates, diatoms and dinoflagellates in the nanoplankton (2–20 μm) size category were examined by epifluorescence microscopy (Olympus BX-60) in 50–150 ml subsamples preserved with glutaraldehyde, stained with the fluorochromes DAPI (Coleman, 1980) or DAPI + proflavin (e.g., Verity and Sieracki, 1993), and mounted on 0.8-μm black Poretics filters. Microplankton (>20 μm) samples were preserved with Lugols' iodine solution or buffered paraformaldehyde and counted by inverted microscopy (Olympus IMT-2). For both nano- and microplankton analyses, diatom and flagellate biovolumes were converted to carbon biomass using modified Strathmann equations (Eppley et al., 1970). *Phaeocystis* cells were enumerated in motile and non-motile categories, the latter including cells occurring in a sheet-like gelatinous matrix or as spherical, ellipsoid and cylindrical colonies. Because they aligned two-dimensionally, individual motile and "sheet-associated" cells were counted on nanoplankton slides. Three-dimensional colonies were counted and measured (colony volumes) in settled microplankton samples, and their volumes were used to estimate cell abundances according to the relationship $\log_{10}$ (cell number) $= 3.61 + 0.51\log_{10}$ (volume, mm^3) from Rousseau et al. (1990). A cellular carbon content of 13.5 pg C $cell^{-1}$ was used for all Phaeocystis cells (Rousseau et al., 1990). Because most (55–95%) of these cells occurred in the sheet form, which could not be measured accurately for mucus volume, the carbon associated with colony mucus was not included in biomass calculations.

Phytoplankton abundances and chlorophyll concentrations were relatively constant within predawn samples from the mixed layers at each station (e.g., Table 1); therefore, mixed-layer C : Chl *a* estimates were based on the mean values of all carbon biomass and pigment estimates within this depth strata. At stations where the euphotic zone was not fully contained within the mixed layer, additional C : Chl *a* ratios were calculated for all depths where the relevant data were available and interpolated for the experimental depths between them.

2.4. Rate estimates

To derive phytoplankton community (Chl *a*) and population-specific rate estimates from dilution experiments, net instantaneous growth rates were calculated for each natural and diluted treatment (k_{nat} and k_{dil}, respectively) from measured changes in Chl *a* and picoplankton abundances during the incubations. Growth rates (μ) were assumed to be the same in both treatments, and mortality rates (m) were assumed to vary proportionately with the dilution of grazer densities (Landry and Hassett, 1982). Thus, specific growth rates and mortality due to grazing were calculated by solving the following two equations:

$$k_{nat} = \mu - m,$$

$$k_{dil} = \mu - 0.31\, m,$$

for the two unknowns, μ and m (Landry et al., 1984). Carbon production rates of individual picoplankton populations were calculated from their growth rate estimates (μ, d^{-1}) and initial estimates of their carbon biomass (B_0 = abundances times cellular carbon contents) according to Vaulot et al. (1995):

$$\text{Carbon production} = B_0(e^{\mu} - 1).$$

Rates of phytoplankton gross carbon production (GCP) were estimated from ^{14}C-uptake measurements multiplied times 2.4, the mean relationship between ^{18}O estimates of gross primary production and ^{14}C production rates from contemporaneous incubations at the same group of stations during July 1995 (SW Monsoon) (Dickson et al., 1999, to be submitted for publication). Additional estimates of phytoplankton community growth rates were computed from the measured rate of ^{14}C-primary production (^{14}CPP) and the calculated GCP per Redalje and Laws (1981):

$$\mu_{CCP} = \ln((C_0 + {}^{14}\text{CPP})/C_0),$$

$$\mu_{GCP} = \ln((C_0 + \text{GCP})/C_0),$$

where C_0 is the initial value for phytoplankton standing stock computed from Chl a concentrations and C : Chl a ratios.

Depth-integrated production estimates were computed from depth profiles according to the trapezoidal rule. Mean euphotic zone rates of growth (μ_z) and grazing mortality (m_z) were determined as biomass-weighted averages to account for variations in phytoplankton Chl a or population abundances in the depth profiles.

3. Results

3.1. Phytoplankton community characteristics

The six experimental stations spanned a broad gradient in environmental conditions, with near-surface NO_3 and Chl a concentrations varying from 0.01 to 11.5 μM and 0.16 to 1.50 μg l^{-1}, respectively (Table 1). NO_3 was low in the mixed layers of the three most offshore stations (N7, S15, S11) and increased approaching the upwelling region along the Omani coastline. Chlorophyll a concentrations were lowest at N7 and S15, intermediate at the high nutrient coastal stations, and highest at S11 where nitrate reached very low levels.

Prochlorococcus were only abundant at the stations characterized by low NO_3 and low Chl a, averaging 158,000 and 264,000 cells ml^{-1} in the mixed layers at stations N7 and S15, respectively (Table 1). *Synechococcus* abundances were typically in the range 40,000–50,000 cells ml^{-1} in the upper euphotic zone at all stations, except for an abundance maximum (123,000 cells ml^{-1}) at station S7 and 80,000 cells ml^{-1} at N7. Abundances of picoeukaryotic algae increased with nutrient concentrations, ranging from approximately 2500–3500 cells ml^{-1} at offshore stations with negligible NO_3 to $>$ 17,000 cells ml^{-1} at the richest coastal station (S2).

Phytoplankton community carbon more than doubled from 29–30 μg C l^{-1} at stations N7 and S15 to 76 μg C L^{-1} at coastal station S2 (Table 2). Combined

Table 2
Carbon-to-chlorophyll ratios averaged over the mixed layer and from below the mixed layer to 1% PAR_0 for each station

Station	Depth (m)	Chl *a* ($\mu g\,l^{-1}$)	Flow cytometry ($\mu g\,C\,l^{-1}$)			Microscopy ($\mu gC\,l^{-1}$)				Total	C:CHL	
			PRO	SYN	PEUK	FLAG	DINO	DIAT	MPHAEO	CPHAEO	($\mu g\,C\,l^{-1}$)	
N7	MLD = 48	0.18	9.3	13.8	2.5	0.4	2.1	1.2	0.3	0.8	30.4	169
	50–75	0.52	5.1	0.7	3.0	2.7	0.4	1.9	0.1	0.7	14.6	28
S15	MLD = 100	0.23	14.2	9.0	3.1	0.3	0.8	0.0	0.1	1.0	28.5	1240
S11	MLD = 74	1.27	0.0	7.0	3.3	1.6	2.3	10.3	0.2	14.6	39.3	31
S7	MLD = 54	0.93	0.0	20.7	7.9	2.9	2.3	4.9	0.5	9.3	48.5	52
	55–80	0.37	0.0	0.3	1.5	0.2	0.3	0.2	0.0	3.3	5.8	16
S4	MLD = 22	0.69	0.0	8.7	13.0	2.7	3.3	30.8	0.9	2.4	61.8	90
	25–40	0.64	0.0	2.5	5.8	1.5	0.8	4.9	0.2	0.3	16.0	25
S2	MLD = 14	0.62	0.0	9.4	17.9	4.3	3.0	38.4	0.2	3.2	76.4	123
	20–50	0.86	0.0	5.2	18.3	5.0	1.7	10.8	1.7	2.2	44.9	52

Note: The mixed layer depth is defined as the depth at which sigma-theta is 0.125 kg m^{-3} larger than surface sigma-theta. The mixed layer included the 1% light level at stations S15 and S11. Estimates of carbon attributed to *Prochlorococcus* (PRO), *Synechcococcus* (SYN), and picoeukaryotes (PEUK) were derived from flow cytometry and carbon per cell conversion factors. Carbon contributions from flagellates (FLAG), dinoflagellates (DINO), diatoms (DIAT), motile *Phaeocystis* (MPHAEO), and colonial *Phaeocystis* (CPHAEO) were estimated from microscopy and carbon per cell conversion factors as described in text.

picoplankton (*Prochlorococcus*, *Synechococcus* and picoeukaryotes) represented 84-92% of mixed-layer community carbon at the more oligotrophic stations (N7 and S15), 23–35% at coastal stations (S2 and S4), and 59% at intermediate station S7. Picoplankton contributed only 26% to community biomass at the high-chlorophyll, low-nutrient station (S11), comparable to that at the coastal eutrophic stations. *Prochlorococcus* was the single most important contributor to phytoplankton carbon at S15 (50%); *Synechococcus* was the largest contributor at stations N7 (45%) and S7 (43%); and diatoms represented half of the community carbon at the coastal stations (S2 and S4). The mid-transect station S11 was characterized by high concentrations of *Phaeocystis* (38% of cell biomass), 95% in nonmotile sheet form. *Phaeocystis* sheet colonies were also relatively abundant at S7 (19% of phytoplankton carbon).

C : Chl *a* ratios for the mixed-layer communities varied from 124 to 169 for the most oligotrophic stations (N7 and S15), from 90 to 123 at diatom-dominated coastal stations (S4 and S2), and from 31 to 52 at stations (S11 and S7) with abundant *Phaeocystis* (Table 2). Where the mixed-layer did not contain all experimental depths to the 1% light level, C : Chl *a* estimates for the lower euphotic zone varied from 16 to 52, representing 17 to 42% of the mixed-layer ratios.

3.2. Community growth rates

Growth rate inferences from ^{14}C-uptake rates and C : Chl *a* ratios were similar in magnitude at the two low-nutrient, low-chlorophyll stations, N7 and S15, with no distinct maxima (Fig. 2). Although the profiles were similarly shaped, depth-integrated growth was higher at station N7 than S15 ($\mu_z = 0.59$ and $0.44\ d^{-1}$, respectively) (Table 3). Growth rates at both stations S11 and S7 exceeded $1.0\ d^{-1}$ at light levels above 27% PAR_0 and decreased to less than $0.1\ d^{-1}$ at 1% PAR_0 (Fig. 2). Integrated growth rate estimates were highest at these two stations, reaching $\mu_z = 1.17\ d^{-1}$ at S11 and $0.84\ d^{-1}$ at S7 (Table 3). Growth rate estimates were lower and showed comparable depth profiles and integrated averages ($\mu_z = 0.63, 0.65\ d^{-1}$) at the two high-nutrient stations, S2 and S4 (Table 3).

Chl *a*-based estimates of community growth and grazing were made from dilution experiments at all stations, except N7 (Fig. 2). At low-nutrient stations S11 and S15, Chl *a* growth (i.e., pigment synthesis rate) was relatively low near the surface but showed a subsurface maximum of 0.7 to $1.0\ d^{-1}$ at approximately the depth of the 7% light level. Grazing losses exceeded synthesis rates in the upper euphotic zone at these stations while growth exceeded grazing in the lower half. Depth-integrated estimates of growth and grazing varied somewhat between stations, with $\mu_z = 0.53$ to $0.55\ d^{-1}$ and $m_z = 0.50$ to $0.37\ d^{-1}$ at stations S11 and S15, respectively. On average, however, microzooplankton grazing accounted for the utilization of about 81% of phytoplankton community growth at these low-nutrient stations.

At the higher-nutrient stations, Chl *a* growth estimates were enhanced in the upper euphotic zone, approaching rates of $1.5\ d^{-1}$ at or above the 27% PAR_0 light depth (Fig. 2). Corresponding estimates of grazing mortality showed a considerable excess of Chl *a* synthesis over grazing losses at the higher light levels, approaching a balance lower in the euphotic zone. Depth-integrated growth rates ranged from 0.91–$1.05\ d^{-1}$

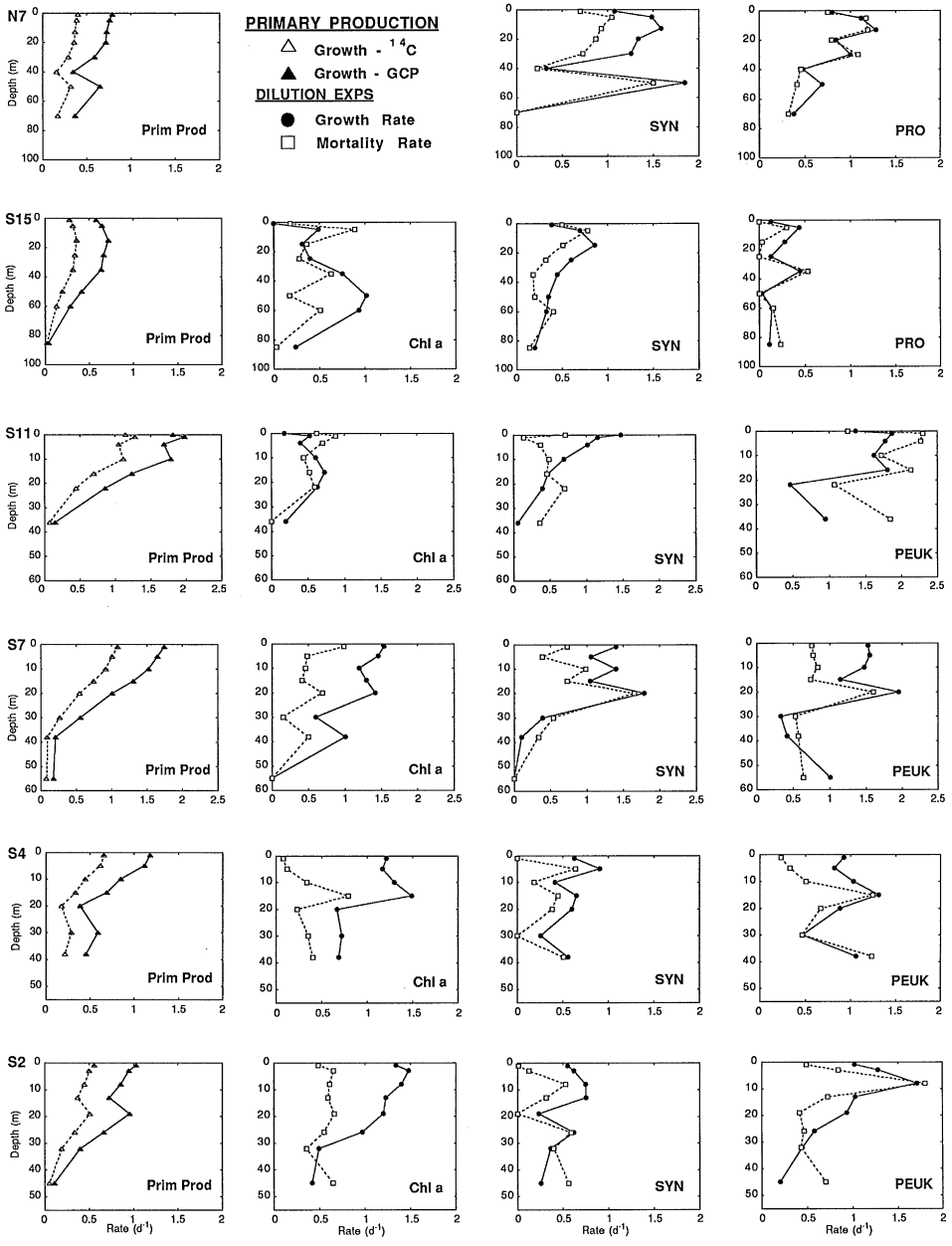

Fig. 2. Growth and mortality rate estimates (d^{-1}) for experimental stations. Growth rates derived from ^{14}C-uptake experiments and estimated gross carbon production (GCP) based on measured carbon : chlorophyll ratios as described in text. Specific growth and losses due to grazing of bulk chlorophyll, *Prochlorococcus*, *Synechococcus*, and picoeukaryotes from in situ dilution experiments. All rate estimates are based on 24-h incubations.

Table 3
Mean rates of phytoplankton growth (μ_z (d^{-1})) and microzooplankton grazing (m_z, (d^{-1})) at six stations during the 1995 SW Monsoon

		Growth rates (μ_z (d^{-1}))				Grazing loss rates (m_z (d^{-1}))			
Station	^{14}C	Chl *a*	PRO	SYN	PEUK	Chl *a*	PRO	SYN	PEUK
N7	0.59	—	0.78	1.12	—	—	0.73	0.72	—
S15	0.44	0.55	0.21	0.46	0.16	0.37	0.18	0.34	0.12
S11	1.17	0.53	—	0.58	1.28	0.50	—	0.50	1.72
S7	0.84	1.05	—	0.84	1.00	0.44	—	0.73	0.79
S4	0.65	0.94	—	0.58	0.91	0.34	—	0.33	0.67
S2	0.63	0.91	—	0.66	0.76	0.54	—	0.33	0.63

Note: Phytoplankton community rates are from measured ^{14}C-uptake $\times 2.4$ to adjust for gross production and from total Chl *a* in contemporaneous dilution incubations. Population-specific rates are for *Prochlorococcus* (PRO), *Synechococcus* (SYN) and picoeukaryotes (PEUK) measured by flow cytometry. All estimates are depth-integrated averages for the euphotic zone (to 1% light) weighted for depth variations in standing stock (Chl *a* or population abundances).

for the three high-nutrient stations (S2, S4, S7). Grazing losses averaged 0.44 d^{-1} for these stations, comparable to the mean m_z for the low-nutrient stations, but only accounted for 46% of Chl *a* growth.

For most of the stations, phytoplankton community growth inferences from Chl *a* in dilution incubations exceeded growth rates calculated from gross-production adjusted ^{14}C uptake. On average, the pigment-based rates were 25% higher than ^{14}C rates at picoplankton-dominated stations (S7 and S15) and 44% higher at diatom-dominated stations (S2 and S4) (Table 3). In contrast, production-based estimates exceeded Chl *a* estimates by a factor of 2.2 at S11, where colony-forming *Phaeocystis* were abundant.

3.3. Picoplankton growth and grazing mortality

Depth-profiles of picoplankton growth and mortality rates are presented adjacent to community rate estimates in Fig. 2. At station N7, growth rate estimates for *Prochlorococcus* showed a maximum of 1.28 d^{-1} at 13 m (44% PAR_o) and exceeded one cell division d^{-1} ($\mu_z = 0.78\ d^{-1}$) throughout the euphotic zone (Table 3). At station S15, the most oligotrophic station on the southern transect, growth rates were consistently much lower, not exceeding 0.45 d^{-1} at any depth and averaging 0.21 d^{-1} for the euphotic zone. Grazing mortality of *Prochlorococcus* followed the pattern for growth, with depth-integrated rates of 0.73 and 0.18 d^{-1} at stations N7 and S15, respectively (Fig. 2). On average, grazing accounted for the loss of 90% of *Prochlorococcus* growth at these two stations.

Overall, depth-integrated growth estimates for *Synechococcus* averaged 0.71 d^{-1} (range = 0.46–1.12 d^{-1}), and mortality due to grazing was 70% of growth (range = 50–87%) (Table 3). Growth rates were generally highest in near-surface

incubations at stations, with low to moderate concentrations of dissolved nutrients, exceeding two cell divisions d^{-1} at stations N7, S11 and S7 (Fig. 2). As noted for *Prochlorococcus*, growth rates of *Synechococcus* were much lower at station S15 ($\mu_{max} = 0.86\ d^{-1}$ at 15 m; $\mu_z = 0.46\ d^{-1}$). *Synechococcus* growth also appeared to be depressed at the high-nutrient stations (S4 and S2), with no estimates greater than $0.91\ d^{-1}$, and average $\mu_z = 0.58$ and $0.66\ d^{-1}$ (Table 3). As a general pattern, depth profiles of grazing mortality followed the growth rate trends, but usually there was a substantial excess of growth over grazing in the upper- to mid-euphotic zone and more balanced growth and grazing below (Fig. 2).

At the oligotrophic stations, there was little measurable growth or grazing of picoeukaryotes. The only significant growth at station N7 was at 50 m ($k_{nat} = 0.66\ d^{-1}$), the depth of the chlorophyll maximum. Station S15 showed low net growth at all depths (range = 0.03–0.31 d^{-1}; $\mu_z = 0.24\ d^{-1}$). Along the other southern transect stations, growth rates tended to be higher offshore, where population abundances were lower, and lower nearshore, where population densities were highest ($\mu_z = 0.76$, 0.91, 1.00 and $1.28\ d^{-1}$ at stations S2, S4, S7 and S11, respectively) (Table 3). At station S11, grazing mortality exceeded growth rates at all but one depth, averaging $1.72\ d^{-1}$ (= 134% of μ_z). At the more coastal stations, depth-integrated grazing losses averaged 0.63 and $0.79\ d^{-1}$ (stations S4 and S7, respectively), accounting for an average of 79% of the growth rate estimates. Except for the most oligotrophic stations (N7 and S15), specific growth rates of picoeukaryotes exceeded those for *Synechococcus* by about 50%, on average. For the same stations, however, mortality rates on PEUK averaged more than double the estimates for SYN (Table 3).

3.4. Changes in cellular fluorescence

Changes in Chl *a* per cell over the course of experimental incubations can provide useful inferences about the in situ light field. Cells that increased in fluorescence per cell may have been held at light levels below that which they were adapted, and vice versa. Chl *a* fluorescence per cell, normalized to standard fluorescent beads, was assessed by flow cytometry from initial and final samples at five of the stations. For a given station, each of the picoplankton groups showed similar initial trends with depth and similar responses to the experimental incubations. Therefore, the fluorescence results for *Synechococcus* illustrate the pattern for the picoplankton as a whole (Fig. 3). At stations N7, S11 and S7, initial measurements of cellular fluorescence were constant throughout the euphotic zone, which was generally contained within a deep surface-mixed layer. At stations S4 and S2, the shallower mixed layers were evident as sharp breaks in the initial distributions of red fluorescence, with near-constant values extending to the depth of the mixed layer and increasing values below.

Red fluorescence per cell was constant over the course of the experimental incubation for near-surface samples at N7, as well as for the deepest sample. Samples from mid-depths, however, showed some increase during incubation, particularly the sample incubated at 40 m. Experimental bottles from station S11 were incubated on shipboard, and only the near-surface samples changed appreciably, showing a decrease in cellular fluorescence over the course of the incubation. Near-surface samples

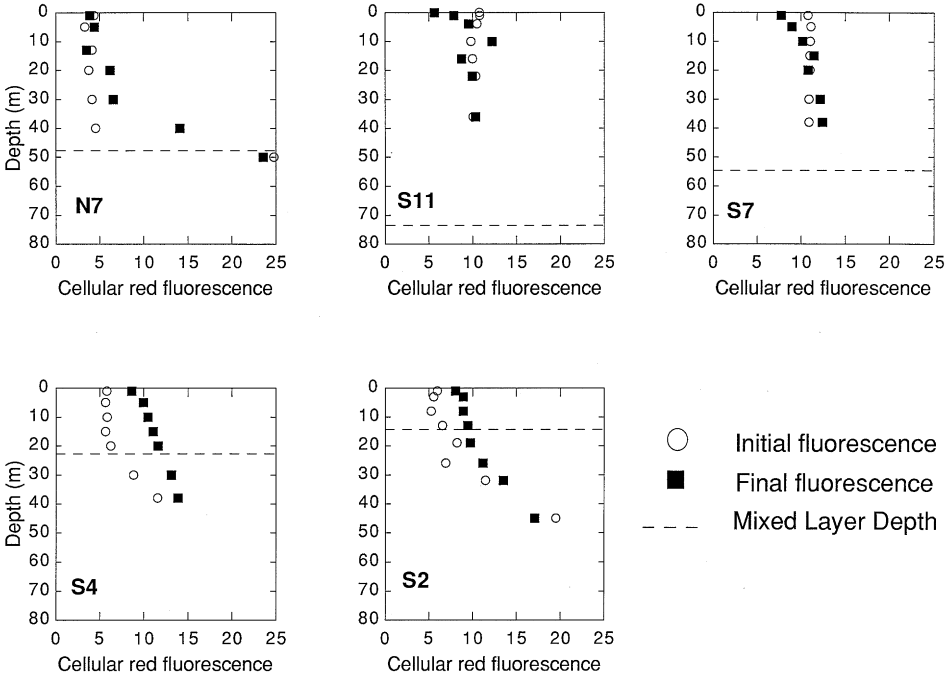

Fig. 3. Changes in the cellular red (chlorophyll) fluorescence of *Synechococcus* during in situ dilution incubations. Fluorescence normalized to 0.57-μm Fluoresbrite beads and presented in arbitrary units. The dotted line represents the mixed layer depth at which sigma-theta is 0.125 kg m^{-3} larger than surface sigma-theta.

from station S7 exhibited less fluorescence after the incubation period while deeper samples showed an increase. In contrast, samples from stations S4 and S2 showed marked increases in cellular fluorescence after the incubation period, with the largest increases occurring in the mixed layer.

3.5. *Contribution of picoplankton to primary productivity*

Estimates of the contributions of each picoplankton group to total gross carbon production (GCP) are presented for specific incubation depths in Table 4, and as depth-integrated totals in Table 5. Picoplankton contributed most to depth-specific production in the upper- to mid-euphotic zone at station N7, exceeding GCP estimates by 10–150% in the upper 30 m (Table 4). At the other stations, the picoplankton contribution either showed no depth pattern (S15, S11 and S2) or peaked in the mid- to lower-euphotic zone (S7, S4).

Depth-integrated production estimates for the total picoplankton community varied from 150 (N7) to 16% (S11) of GCP, but were more typically 40–60% of GCP (Table 5). At the more oligotrophic stations N7 and S15, nearly all picoplankton

Table 4
Contributions of picophytoplankton to primary production. All values reported as mmol C m^{-3} d^{-1}

Station	Depth	%I	GCP	PRO	SYN	PEUK	Total	%Pico
N7	1	93	2.9	0.9	2.3	0	3.2	110
N7	5	75	2.7	1.5	3.8	0	5.3	196
N7	13	44	2.4	1.7	4.2	0	5.9	246
N7	20	27	2.4	0.9	3.1	0	4	167
N7	30	15	1.9	1.2	2.7	0	3.9	205
N7	40	7	1.7	0.7	0.5	0	1.2	71
N7	50	4	1.6	0.4	0.6	0.4	1.0	63
N7	70	1	0.3	0.2	0	0	0.2	67
S15	1	93	1.8	0.2	0.4	0	0.6	33
S15	5	75	2.0	0.7	0.8	0.1	1.5	75
S15	15	44	2.4	0.4	1.0	0.1	1.4	58
S15	25	27	2.4	0.2	0.6	0	0.8	33
S15	35	15	2.1	0.7	0.4	0	1.1	52
S15	50	7	1.2	0	0.3	0	0.3	25
S15	60	4	0.8	0.2	0.3	0	0.5	63
S15	85	1	0.1	0.1	0.2	0	0.3	300
S11	0	100	19.7	0	3.9	0.6	4.5	23
S11	0	100	20.0	0	2.1	0.8	2.9	15
S11	1	90	22.7	0	1.4	1.5	2.9	13
S11	4	56	15.9	0	1.1	1.6	2.7	17
S11	10	29	14.2	0	0.6	1.2	1.8	13
S11	16	14	7.8	0	0.4	1.5	1.9	24
S11	22	8	4.4	0	0.3	0.2	0.5	11
S11	36	2	0.4	0	0	0.2	0.2	50
S7	1	93	19.0	0	5.5	2.5	8.0	42
S7	5	75	17.0	0	3.3	2.7	6.0	35
S7	10	44	14.6	0	5.3	2.3	7.6	52
S7	15	27	11.0	0	3.1	1.4	4.5	41
S7	20	15	7.0	0	8.6	3.6	12.2	174
S7	30	7	2.8	0	0.8	0.3	1.1	39
S7	38	4	1.0	0	0.2	0.3	0.5	50
S7	55	1	0.1	0	0	0.2	0.2	200
S4	1	93	9.5	0	0.7	1.6	2.3	24
S4	5	75	9.3	0	1.1	1.5	2.6	8
S4	10	44	7.2	0	0.4	1.9	2.3	32
S4	15	27	5.1	0	0.7	3.1	3.8	75
S4	20	15	3.1	0	0.5	1.5	2.0	65
S4	30	7	1.4	0	0.1	0.4	0.5	36
S4	38	4	0.5	0	0.1	0.5	0.6	120
S2	1	93	10.3	0	1.2	2.5	3.7	36
S2	3	75	9.2	0	1.1	3.6	4.7	51
S2	8	44	8.4	0	1.1	5.4	6.5	77
S2	13	27	8.4	0	1.5	3.1	4.6	55

Table 4 (Continued)

Station	Depth	%I	GCP	PRO	SYN	PEUK	Total	%Pico
S2	19	15	5.4	0	0.5	2.6	3.1	57
S2	26	7	3.2	0	0.2	3.1	1.5	47
S2	32	4	2.2	0	0	0.8	0.8	36
S2	45	1	0.6	0	0	0.5	0.5	83

Note: Production represents ^{14}C carbon assimilation $\times 2.4 \sim$ gross carbon production (GCP). PRO, SYN, and PEUK refer to carbon assimilation attributed to *Prochlorococcus*, *Synechococcus*, picoeukaryotes and total picoplankton. Values are based on specific growth rates, standing stocks and estimates of carbon per cell. All comparisons are based on 24-h incubations

Table 5
Depth-integrated estimates of gross carbon production GCP, (mmol C $m^{-2} d^{-1}$) from ^{14}C-uptake experiments and cell specific rates from dilution experiments

Station	GCP	Pro	Syn	Peuks	% Total
N7	123	58	126	< 1	150
S15	122	25	39	6	57
S11	305	0	18	30	16
S7	334	0	142	71	64
S4	160	0	17	52	43
S2	211	0	23	95	56

Note: Picophytoplankton production estimates based on specific growth rates (μ), initial cell densities, and carbon per cell conversion factors as described in text. % Total represents the fraction of ^{14}C-uptake attributed to the combined picoplankton populations

production was due to *Synechococcus* and *Prochlorococcus*. *Prochlorococcus* was effectively absent at the other stations, while *Synechococcus* contributed substantially at S7 (43% of GCP) but only modestly (< 11% of GCP) elsewhere. In contrast, picoeukaryote production increased in relative terms from offshore to coastal stations, reaching a high of 45% of GCP at S2.

4. Discussion

4.1. Picoplankton dynamics

The present study was part of an investigation of the dynamics of picoplankton populations in the Arabian Sea under different conditions of environmental forcing and within the context of community-level assessments of primary production, phytoplankton growth and microzooplankton grazing. We were interested in documenting the rates of growth and grazing on target phytoplankton populations, understanding how they varied among stations with different environmental

characteristics, and testing the internal consistency of results and interpretations from alternative methods.

At the time that this study was undertaken, it was expected that the strong diel synchrony in *Prochlorococcus* cell division (Vaulot et al., 1995) limited its maximum growth rate to one division per day. If this were the case, *Prochlorococcus* would be effectively excluded from marine environments where the protistan grazing impact on bacterial-sized prey substantially exceeded 0.7 d^{-1}. Based on the results of this study as well as others, however, there appears to be no such constraint on *Prochlorococcus* growth potential, at least for the strain(s) residing in the Arabian Sea. Reckermann and Veldhuis (1997) reported *Prochlorococcus* growth rates ranging up to 2.2 d^{-1} in the Gulf of Aden during the 1992–1993 NE Monsoon. The highest estimate from the present study, 1.28 d^{-1} at station N7 (Fig. 2), is also consistent with rate estimates of 1.16–1.29 d^{-1} from cell cycle analysis of diel samples collected from the 10–25 m depth strata at N7 during the same cruise (Liu et al., 1998). The excellent agreement between these two entirely independent approaches – one involving incubation of contained populations, the other requiring no experimental manipulation at all – lends strong support to the notion that *Prochlorococcus* can achieve growth rates up to 2 cell divisions d^{-1}. Consequently, the virtual absence of *Prochlorococcus* at stations with higher nutrients cannot be explained by their inability to grow fast when environmental conditions are appropriate. Since *Prochlorococcus* are also unlikely to suffer disproportionately high grazing losses relative to other picophytoplankton because of their relatively small size, the explanation for their low abundances at four of our six stations must therefore reside in some, as yet undiscovered, growth requirement or inhibitory factor that affected the quality of the growth environment at stations S2–S11. In this latter regard, reduced growth rates of *Synechococcus* and picoeukaryotes were evident at the higher-nutrient coastal stations (S2 and S4) in our data (Table 3), and Burkhill et al. (1993) also showed a decrease in *Synechococcus* growth rates at stations close to the Omani coast.

The striking difference in growth rates of *Prochlorococus* and *Synechococcus* at stations N7 and S15 is another interesting puzzle because these stations superficially appear to provide similar growth environments in terms of light, temperature and macronutrients. Based on inferences from shipboard ADCP measurements of current patterns (Flagg and Kim, 1998; Campbell et al., 1998), station N7 resided in a cyclonic (upwelling) mesoscale eddy which may have enhanced the rate of supply of nutrients to the euphotic zone. Even if upwelling explained the higher growth rates of ambient populations at N7, however, it could not have brought new nutrients to the contained populations during the incubation experiments. Thus, the higher picoplankton growth rates for the station may have reflected a more favourable recent nutrient history, rather than the conditions in the incubation bottles. Along these lines, the lower growth rates at station S15 might involve different species or clones, or population adaptations to water masses with different histories. Based on T–S signatures, for example, the water mass at S15 was of distinctly different origin than the rest of the stations studied (Morrison et al., 1998).

Even though the experiments at station S11 were incubated on shipboard, we assume that they can be compared to in situ experiments because the cellular Chl *a*

fluorescence of incubated populations revealed no problems with simulated light levels (Fig. 3). Colonies of *Phaeocystis* sp. reached a biomass maximum at S11 (Garrison et al., 1998), which could account for the enhanced Chl *a* concentrations and high primary production at this station. The combination of low Chl *a*-based growth rates and low nutrient concentrations suggests that the *Phaeocystis* colonies may have been approaching or even in a state of senescence and decline. The recent history of water at S11 presumably involved high nutrients, which were subsequently exhausted by the accumulation of *Phaeocystis* biomass. In fact, physical oceanographic observations suggest the community at S11 was likely an advanced successional phase of a coastally derived bloom advected there as the offshore extension of a coastal filament (Flagg and Kim, 1998; Manghnani et al., 1998). Such a history would explain the absence of *Prochlorococcus*, despite low nutrient conditions which generally favor its dominance (Campbell et al., 1998). The large discrepancy between ^{14}C and Chl *a* estimates of growth rate at this station presumably reflected the production of extracellular mucus not accounted for in our C : Chl *a* ratios (see discussion below).

Community rate estimates from the in situ mini-dilutions were in good agreement with results of standard dilution experiments incubated on shipboard (Landry et al., 1998). Average mortality rates due to grazing from each of the two approaches never differed by more than $0.07\ d^{-1}$ at a given station, and they exhibited similar trends in the relationships of growth to grazing, with a closer balance at the oligotrophic sites and substantial excess of growth over grazing at the high-nutrient stations. The excess growth at the high-nutrient stations is consistent with the enhanced abundance of large diatoms, which are less likely to be grazed by small protozoans (Edwards et al., 1999; Landry et al., 1998).

Within the picoplankton, losses to microzooplankton grazing tended to be more closely coupled to growth rates, with grazing accounting for averages of 90, 70 and 86% of the growth rates for *Prochlorococcus*, *Synechococcus* and picoeukaryotic algae. Over the depth-integrated euphotic zone, the observed net rates of growth of these populations averaged 0.04, 0.22 and $0.05\ d^{-1}$, respectively. A generally good balance between growth and grazing has been noted for previous studies of picoplankton dynamics in the Arabian Sea, but the data set is limited (Burkhill et al. (1993), (3 experiments), Reckermann and Veldhuis (1997) (6 experiments)). In contrast, for six stations along the Somali coast at which net growth rates were measured in in situ incubations at seven depths during the 1992–1993 SW Monsoon, Veldhuis et al. (1997) reported average μ_{net} of 0.34, 0.32 and $0.37\ d^{-1}$ for *Prochlorococcus*, *Synechococcus* and small picoeukaryotic algae, respectively. Thus, a close balance between growth and grazing losses appears to be fairly typical for picoplankton populations in the Arabian Sea. However, significant departures from this balance can occur as the populations respond to changing conditions in this highly dynamic system.

Over the depth ranges of integration and the stations at which they could be directly compared, growth and grazing rate estimates for *Prochlorococcus* averaged 76% of the mortality rates for *Synechococcus*, and picoeukaryote rates were 1.7 times as high as *Synechococcus*. If we assume that the diameters of *Prochlorococcus*, *Synechococcus* and picoeukaryotes were 0.7, 1.0 and 2.0 μm, respectively, the mean

rates for the different picoplankton groups increased roughly with the first power of prey diameter. Theoretical predictions of prey vulnerability to flagellates feeding randomly by direct particle interception follow a similar size dependence (Monger and Landry, 1990,1991). Thus, while considerable variability is evident in individual depth profiles, the mean dynamics of picophytoplankton populations in the Arabian Sea appear to be linked by size and consistent with grazing control by common flagellate predators.

4.2. Growth and production rate estimates from different methods

This is the first study to our knowledge that has looked at relationships between growth and production rate inferences from dilution and ^{14}C-uptake experiments from contemporaneous in situ incubations. Since these techniques measure different properties of the contained phytoplankton community – the specific growth rates of the Chl *a*-bearing organisms versus the net accumulation of labeled-particulate carbon – we had no a priori expectation that they should agree closely. Nonetheless, we attempted to minimize some of the obvious problems in comparing results from these different methods. For example, given that a perfect balance of growth and grazing during the incubations would yield no net change in cell abundance (i.e., $\mu_{net} = \mu - g = 0$), the Δ cell carbon method of comparing net population growth to ^{14}C production (Veldhuis et al., 1997) would provide conservative assessments of picoplankton contributions to production. The direct comparison of specific growth (μ) rates to phytoplankton gross production avoids this problem. Despite our attempts to account for station-to-station and depth variability in C : Chl *a* ratios, however, uncertainties in carbon biomass conversions remain problematic in comparing results from pigment-, population- and production-based methodologies. Different facets of the biomass conversion problem are illustrated in our results from different stations.

First, the high estimates of picoplankton production, which exceeded 150% of gross production estimates at station N7 (Table 5), suggest that picoplankton cellular carbon contents may have been set too high. As noted previously, our estimates were on the low end of values applied to picoplankton in the marine environment (53, 175 and 975 fg C cell^{-1} for PRO, SYN and PEUK, respectively). However, values of about a factor of two lower (25, 98 and 586 fg C cell^{-1}) can be computed from the 140 fg C μm^{-3} conversion factor of Hagström et al. (1988) and the spherical biovolumes of 0.7 μm (0.065 μm^3), 1.1 μm (0.70 μm^3) and 2.0-μm (4.2 μm^3) diameter cells. These lower values would bring our calculated picoplankton production rates in line with estimated GCP at station N7. They would mean, however, that our assessments of picoplankton contributions to total phytoplankton community biomass and production could be exaggerated by as much as a factor of 2. If so, perceptions of the relative importance of picophytoplankton in the marine environment, not only from this study but others as well, might be systematically biased by the widespread use of high cellular carbon conversion estimates.

Errors in the carbon contents of individual picoplankton cells also influence the comparison of Chl *a* and ^{14}C community-level growth rates by inflating the calculated

C : Chl *a* and, hence, the initial community carbon estimates used to derive μ from GCP. Thus, the generally lower μ_z estimates from ^{14}C-uptake compared to Chl *a* growth in dilution incubations could be another indication of overestimated cellular carbon contents. However, a second problem with biomass conversions in the present study is evident from the low C:Chl *a* estimates for station S11, and to a lesser extent S7 (Table 2). These estimates may or may not accurately reflect the C : Chl *a* ratios of the photosynthetically active biomass, but in failing to account for the mucus content of *Phaeocystis* colonies, they clearly underestimate the amount of carbon that must be produced for the community to double itself in biomass. The direction and magnitude of the discrepancy in GCP and Chl *a* growth rate estimates for station S11 suggest that much of the measured carbon production at this station is in the form of mucus.

Finally, changes in C : Chl *a* due to pigment photoadaptation is another factor that can confound comparisons of community growth rate estimates from ^{14}C-uptake and dilution incubations. Observed changes in cellular fluorescence (Fig. 3) allow us to quantify the possible magnitudes of this effect for various experiments. Clearly, the net effect for offshore stations S7 and S11 would be little, other than the fact that photobleaching in the near-surface samples might call for an upward adjustment of pigment-based estimates for these depths. In contrast, the marked increases in cellular fluorescence at coastal stations S2 and S4 have potentially large effects on the rate estimates. At station S2, cellular fluorescence increased on average by 40% in the depth-integrated profile; at station S4, fluorescence was enhanced by 55%. Although other dominant phytoplankton groups (e.g., diatoms) may have responded differently, if we assume that the pigment response of *Synechococcus* was typical, growth in pigment per cell, as opposed to true growth of new cells, could explain the higher ratios of μ_z estimates from Chl *a* and GCP approaches at stations S2 and S4 (1.45) relative to S7 and S15 (1.25).

4.3. Picoplankton contributions to primary production and community biomass

As noted above, assessing the contributions of picoplankton populations to community biomass and production needs to be done cautiously because of the still considerable uncertainty in cellular carbon contents. One way that we can minimize errors from these uncertainties is to compare estimates of the biomass and production contributions to one another, since both are affected in the same direction, though not exactly to the same extent, by carbon conversion errors. *Prochlorococcus* contributed more to production than biomass at station N7 and less at S15, with about equal contributions overall at these oligotrophic sites (Table 6). *Synechococcus* accounted for significantly more production relative to its biomass at N7 and less production to biomass at coastal station S2 and S4. On average, however, *Synechococcus* contributed about equally to production and biomass across the range of environmental conditions. In contrast, picoeukaryotes showed a clear trend in reduced production relative to biomass in the offshore, oligotrophic stations and enhanced production to biomass contributions in the high-nutrient coastal stations, with a 28% higher contribution to production for the 6 station average. Due to the shift in community

Table 6
Estimated percentage contributions of picophytoplankton to total phytoplankton community biomass and primary production

	PRO		SYN		PEUK		Total PICO	
Station	Biomass	Prod	Biomass	Prod	Biomass	Prod	Biomass	Prod
N7	30.6	47.2	45.4	102.0	8.2	< 1.0	84.2	150.0
S15	49.8	20.5	31.6	32.0	10.9	4.9	92.3	57.4
S11	—	—	17.8	5.9	8.4	9.8	26.2	15.7
S7	—	—	42.7	42.5	16.3	21.3	60.0	63.8
S4	—	—-	14.1	10.6	21.0	32.5	35.1	43.1
S2	—	—	12.3	10.9	23.4	45.0	35.7	56.0

Note: Biomass percentages are computed from data in Table 3; production (Prod) contributions are from Table 5.

dominants and activity levels, from prokaryotes offshore to picoeukarytotes nearshore, picophytoplankton as a whole contributed disproportionately to production at only the oligotrophic (N7) and eutrophic (S2 and S4) extremes of the experimental stations.

Because they achieve extraordinary numerical abundances in certain environments, the importance of photosynthetic prokaryotes, *Prochlorococcus* and *Synechococcus*, is usually recognized and perhaps even sometimes overstated. In comparison, the eukaryotic picoplankton are not numerically dominant in the open oceans and are easily overlooked relative to larger phytoplankton in richer habitats. As demonstrated by Li (1994), however, larger size and high cell-specific rates of ^{14}C uptake allow picoeukaryotic algae to be important, despite lower abundances. The present study suggests that picoeukaryotes are particularly abundant and disproportionately productive in coastal marine systems. Even during intense monsoonal forcing in the Arabian Sea, picoeukaryotic algae appear to account for a large portion of primary production in the coastal upwelling regions. This production supports an active community of protistan grazers in the upwelling region, explaining high rates of loss to microzooplankton grazing (Landry et al., 1998) and relatively modest carbon export fluxes in these areas (Buesseler, 1998; Buesseler et al., 1998).

In summary, the present study demonstrates that picophytoplankton were a dynamic and important component of the plankton community in the Arabian Sea during the 1995 SW Monsoon. Although the general magnitudes of population growth and mortality rates and their interrelationships are now reasonably well documented by this study and others, additional work is needed to understand why the different populations vary so greatly in relative abundances among stations, how apparently comparable conditions at different stations lead to widely different growth responses, and to better constrain estimates of the contributions of picophytoplankton to measured rates of community primary production.

Acknowledgements

This study was supported by NSF grants OCE 93-11246 (to MRL and LC), -12355 (to RTB), and -10634 (to DLG and MMG). We gratefully acknowledge the assistance of all our colleagues and the captain and crew of the R.V. *Thomas G. Thompson*. In particular, we thank the hydrographic team, led by J. Morrison and L. Codispoti, and Project Coordinator, S. L. Smith. This paper is contribution no. 430 from the U.S. JGOFS Program and no. 4783 from the School of Ocean and Earth Science and Technology, University of Hawaii at Manoa, Honolulu, USA.

References

Brock, J.C., McClain, C.R., 1991. Interannual variability in plankton blooms observed in the northwestern Arabian Sea during the southwest monsoon. Journal of Geophysical Research 97, 733–750.

Buessler, K., 1998. The decoupling of production and particulate export in the surface ocean. Global Biogeochemical Cycles 12, 297–310.

Buessler, K., Ball, L., Andrews, J., Benitez-Nelson, C., Belastock, R., Chai, F., Chao, Y., 1998. Upper ocean export of particulate organic carbon in the Arabian Sea derived from Thorium-234. Deep-Sea Research II 45, 2461–2488.

Burkhill, P.H., Leakey, R.J.G., Owens, N.J.P., Mantoura, R.F.C., 1993. *Synechococcus* and its importance to the microbial foodweb of the northwestern Indian Ocean. Deep-Sea Research II 40, 773–782.

Campbell, L., Landry, M.R., Constantinou, J., Nolla, H.A., Brown, S.L., Liu, H., Caron, D.A., 1998. Response of microbial community structure to environmental forcing in the Arabian Sea. Deep-Sea Research II 45, 2301–2326.

Campbell, L., Nolla, H.A., Vaulot, D., 1994. The importance of *Prochlorococcus* to community structure in the central North Pacific Ocean. Limnology and Oceanography 39, 954–961.

Chavez, F.P., 1989. Size distribution of phytoplankton in the central and eastern tropical Pacific. Global Biogeochemical Cycles 3, 27–35.

Coleman, A.W., 1980. The use of DAPI for identifying and counting aquatic microflora. Limnology and Oceanography 25, 943–948.

Dickson, M.-L., Orchardo, J., Bender, M., Barber, R.T., Marra, J. McCarthy, J.J., Sambrotto, R.N. 1999. Production and respiration rates in the Arabian Sea during the Northeast and Southwest monsoons. Deep-Sea Research II 46, 843–863.

Edwards, E.S., Burkhill, P.H., Stelfox, C.E., 1999. Zooplankton herbivory in the Arabian Sea during and after the SW Monsoon, 1994. Deep-Sea Research II, in press.

Elliot, A.J., Savidge, G., 1990. Some features of the upwelling off Oman. Journal of Marine Research 48, 319–333.

Eppley, R.W., Reid, F.M.H., Strickland, J.D.H., 1970. Estimates of phytoplankton crop size, growth rate, and primary production. In: Strickland, J.D.H. (Ed.), The ecology of the plankton off La Jolla California in the period April through September, 1967. Bulletin of Scripps Institution of Oceanography 17, 33–42.

Flagg, C.N., Kim, H.-S., 1998. Upper ocean currents in the northern Arabian Sea from shipboard ADCP measurements collected during the 1994–1996 JGOFS and ONR programs. Deep-Sea Research II 45, 1917–1960.

Garrison, D.L., Gowing, M.M., Hughes, M.P., 1998. Nano- and microplankton in the northern Arabian Sea during the Southwest Monsoon, August-September, 1995: A US-JGOFS study. Deep Sea Research II 45, 2269–2300.

Glover, H.E., 1985. The physiology and ecology of the marine cyanobacterial genus *Synechococcus*. Advances in Microbiology 3, 49–107.

Hagström, Å., Azam, F., Andersson, A., Wikner, J., Rassoulzadegan, F., 1988. Microbial loop in an oligotrophic pelagic marine ecosystem: possible roles of cyanobacteria and nanoflagellates in the organic fluxes. Marine Ecology Progress Series 49, 171–178.

Iturriaga, R., Marra, J., 1988. Temporal and spatial variability of chroccoid cyanobacteria *Synechococcus* spp. specific growth rates and their contribution to primary productivity in the Sargasso Sea. Marine Ecology Progress Series 44, 175–181.

Itturiaga, R., Mitchell, B.G., 1986. Chrococcoid cyanobacteria: a significant component in the food web dynamics of the open ocean. Marine Ecology Progress Series 28, 291–297.

Landry, M.R., Brown, S.L., Campbell, L., Constantinou, J., Liu, H., 1998. Spatial patterns in phytoplankton growth and microzooplankton grazing in the Arabian Sea during monsoon forcing. Deep-Sea Research II 45, 2353–2368.

Landry, M.R., Haas, L.W., Fagerness, V.L., 1984. Dynamics of microbial plankton communities: experiments in Kaneohe Bay, Hawaii. Marine Ecology-Progress Series 16, 127–133.

Landry, M.R., Hassett, R.P., 1982. Estimating the grazing impact of marine microzooplankton. Marine Biology 67, 283–288.

Li, W.K.W., 1994. Primary production of prochlorophytes, cyanobacteria, and eucaryotic ultraplankton: measurements from flow cytometric sorting. Limnology and Oceanography 39, 169–175.

Liu, H., Campbell, L., Landry, M.R., Nolla, H.A., Brown, S.L., Constantinou, J., 1998. *Prochlorococcus* and *Synechococcus* growth rates and contributions to production in the Arabian Sea during the 1995 Southwest and Northeast Monsoons. Deep-Sea Research II 45, 2327–2352.

Manghnani, V., Morrison, J.M., Hopkins, T.S., Bohm, E., 1998. Advection of upwelled waters in the form of plumes off Oman during the Southwest Monsoon. Deep-Sea Research II 45, 2027–2052.

Michaels, A.F., Silver, M.W., 1988. Primary production, sinking fluxes, and the microbial food web. Deep-Sea Research 35, 473–490.

Monger, B.C., Landry, M.R., 1990. Direct-interception feeding by marine zooflagellates: the importance of surface and hydrodynamic forces. Marine Ecology-Progress Series 65, 123–140.

Monger, B.C., Landry, M.R., 1991. Prey-size dependency of grazing by free-living marine flagellates. Marine Ecology-Progress Series 74, 239–248.

Monger, B.C., Landry, M.R., 1993. Flow cytometric analysis of marine bacteria with Hoescht 33342. Applied Environmental Microbiology 59, 905–911.

Morrison, J., Codispoti, L.A., Gaurin, S., Jones, B., Manghnani, V., Zheng, Z., 1998. Seasonal variation of hydrographic nutrient fields during the U.S. JGOFS Arabian Sea Process Study. Deep-Sea Research II 45, 2053–2102.

Peinert, R., von Bodungen, B., Smetacek, V.S., 1989. Food web structure and loss rate. In: Berger, W.H., Smetacek, V.S., Wefer, G. (Eds.), Productivity of the Ocean: Present and Past. Wiley, New York, pp. 35–48.

Reckermann, M., Veldhuis, M.J.W., 1997. Trophic interactions between picophytoplankton and micro- and nanozooplankton in the western Arabian Sea during the NE monsoon 1993. Aquatic Microbial Ecology 12, 263–273.

Redalje, G.G., Laws, E.A., 1981. A new method for estimating phytoplankton growth rates and carbon biomass. Marine Biology 62, 73–79.

Rousseau, V., Mathot, S., Lancelot, C., 1990. Calculating carbon biomass of *Phaeocystis* sp. from microscopic observations. Marine Biology 107, 305–314.

Smith, R.L., Bottero, J.S., 1977. On upwelling in the Arabian Sea. In: Angel, M.V. (Ed.), A Voyage of discovery. Supplement to Deep-Sea Research. Pergamon Press, London, pp. 291–304.

Tarran, G.A., Burkhill, P.H., Edwards, E.S., Woodward, E.M.S., 1999. Phytoplankton community structure in the Arabian Sea during and after the SW Monsoon, 1994. Deep-Sea Research II 46, 655–676.

Vaulot, D., Marie, D., Olson, R.J., Chisolm, S.W., 1995. Growth of *Prochlorococcus*, a photosynthetic prokaryote, in the equatorial Pacific Ocean. Science 268, 1480–1482.

Veldhuis, M.J.W., Kraay, G.W., van Bleijswijk, J.D.L., Baars, M.A., 1997. Seasonal and spatial variability in phytoplankton biomass, productivity and growth in the northwestern Indian Ocean: the southwest and northeast monsoon, 1992-1993. Deep-Sea Research I 44, 425–449.

Verity, P.G., Sieracki, M.E., 1993. Use of color image analysis and epifluorescence microscopy to measure plankton biomass. In: P.F. Kemp, et al. (Eds.), Current Methods in Aquatic Microbial Ecology. Lewis, pp. 327–338.

Waterbury, J.B., Watson, S.W., Valois, F.W., Kranks, D.G., 1986. Biological and ecological characterization of the marine unicellular cyanobacterium *Synechococcus*. Canadian Bulletin of Fisheries and Aquatic Sciences 214, 71–120.

Young, D.K., Kindle, J.C., 1994. Physical processes affecting availability of dissolved silicate for diatom production in the Arabian Sea. Journal of Geophysical Research 99, 22619–22632.